



Macroscopic Twinning Strain in Nanocrystalline Cu

F. Wu, Y.T. Zhu & J. Narayan

To cite this article: F. Wu, Y.T. Zhu & J. Narayan (2014) Macroscopic Twinning Strain in Nanocrystalline Cu, Materials Research Letters, 2:2, 63-69, DOI: [10.1080/21663831.2013.862874](https://doi.org/10.1080/21663831.2013.862874)

To link to this article: <https://doi.org/10.1080/21663831.2013.862874>



© 2013 The Author(s). Published by Taylor & Francis.



Published online: 29 Nov 2013.



Submit your article to this journal [↗](#)



Article views: 1875



View related articles [↗](#)



View Crossmark data [↗](#)



Citing articles: 6 View citing articles [↗](#)

Macroscopic Twinning Strain in Nanocrystalline Cu

F. Wu, Y.T. Zhu* and J. Narayan*

Department of Materials Science & Engineering, North Carolina State University, Raleigh, NC 27695, USA

(Received 16 September 2013; final form 2 November 2013)

Most deformation twins in nanocrystalline face-centered cubic (NC fcc) metals are reported to produce zero-macrostrain, which is attributed to either random activation of partials (RAP) or cooperative slip of three partials (CSTP). Here, we report that when the RAP mechanism is suppressed, ~44% twins in NC Cu produced zero-macrostrain via the CSTP mechanism. This indicates that both RAP and CSTP are major mechanisms to generate zero-macrostrain twins. In addition, our results also indicate that stress state affects the twinning mechanism in NC fcc metals, and monotonic activation of partials with the same Burgers vector dominates twin formation under monotonic stress.

Keywords: Twinning Mechanism, Macrostrain, Nanocrystalline fcc Metals, Random Activation of Partial, Cooperative Slip of Three Partial, Monotonic Activation of Partial

Nanocrystalline (NC) materials deform via mechanisms that are different from their coarse-grained counterparts.[1,2] For example, deformation twinning has been frequently observed even in NC face-centered cubic (fcc) materials that do not deform by twinning in their coarse-grained counterparts.[2,3] Formation of twins in NC metals [2,4,5] plays a critical role in their physical and mechanical properties, such as good electrical conductivity, and excellent resistance to current-induced diffusion.[6,7] The interactions between twins and gliding dislocations at twin boundaries (TBs) have been observed both experimentally [7–14] and by molecular dynamics (MD) simulations [15–18] to result in an unusual combination of ultrahigh strength and high ductility.[7,9,19–24] In NC materials, MD simulations [25–27] have predicted that single or multiple deformation twins can be formed by emission of Shockley partial dislocations on adjacent {111} planes from grain boundaries. This formation mechanism has been confirmed later by abundant experimental evidence.[3,28–34]

One of the most salient features of deformation twins in NC fcc metals is that most of them produce very little or even zero macroscopic strain.[23,35–39] A deformation twin is formed by the slip of multiple partials. While the slip of an individual partial produces local strain, the net strain from slips of multiple partials could sum to zero on a macroscopic scale, producing a deformation twin with zero-macrostrain. This is in sharp contrast to

a deformation twin in conventional coarse-grained fcc metals, which is usually produced by the slip of partials with the same Burgers vectors and produce a macroscopic strain. Whether deformation twins in NC metals produce macroscopic strain may have a significant effect on their microstructural evolution and mechanical behavior during tensile testing. For example, it is known that grain rotation [40–42] and grain boundary sliding [40] occur extensively during the deformation of NC metals, which may lead to grain growth. Deformation twins that do not produce macroscopic strain will result in a smooth grain boundary,[23] which will make grain rotation and grain boundary sliding easier. Therefore, it is of great importance to understand how the microstructures and stress conditions affect the formation of twins with zero macroscopic strain.

Two mechanisms have been proposed for deformation twins with zero macroscopic strain. One is the random activation of partials (RAP) mechanism by Wu et al.,[23] in which partial dislocations with different Burgers vectors are randomly activated. The RAP mechanism was proposed to require the change of local stress orientation with time during deformation, so that the resolved shear stress on partials with different Burgers vectors varied with time during the deformation. Grain rotation and grain boundary sliding were believed to promote the RAP mechanism. The other mechanism was proposed by Wang et al. [35–38] and Li et al.,[39] which

*Corresponding authors. ytzhu@ncsu.edu, narayan@ncsu.edu

involved the cooperative slip of three partials (CSTP) with the sum of their Burgers vectors equaling zero, generating twins with zero-macrostrain. This mechanism does not require the variation of local stress orientation. This raises a critical issue: which mechanism plays a major role in the formation of deformation twins with zero-macrostrain in NC fcc metals? To complicate this issue further, monotonic activation of partial (MAP) dislocations with the same Burgers vector was also found in NC fcc metals.[19] Although the MAP twins are in small percentage, they form under the same stress condition as the CSTP twins.

To solve this issue, we suppressed the RAP in NC Cu grains by designing a layer-by-layer microstructure, to deter the grain rotation and grain boundary sliding of NC Cu grains during the deformation. In addition, the nanograins are textured to have their $\{111\}$ planes parallel to the film surface, and the residual stress is oriented to have resolved shear stress on one type of partial dislocations only. Such a microstructure and stress state not only suppresses the RAP mechanisms, but also should promote the CSTP mechanism and the MAP mechanism. This unique experimental design should be able to clarify if CSTP or RAP or both mechanisms play a significant role in the formation of twins with zero-macrostrain. If most twins still produce a zero-macrostrain when RAP is suppressed, the CSTP mechanism should be the dominating mechanism. On the other hand, if only a very small fraction of twins produce zero-macrostrain, the RAP mechanism is likely the dominating mechanism in the previous report,[23] and the MAP mechanism should be dominant mechanism in the current experiment. However, if the fraction of twins that produce zero-macrostrain is close to, but less than, 50%, both RAP and CSTP mechanisms should have played significant roles in the formation of zero-macrostrain twins reported earlier.[23]

Experimental Approach The Cu/Ta multilayer nanostructures were produced using pulsed laser deposition (PLD) in a multi-target stainless-steel chamber using a pulsed KrF excimer laser (wavelength 248 nm, pulse duration 25×10^{-9} s, and repetition rate 10 Hz). The targets were 4N purity Cu sheet and Ta sheet obtained from ESPI Metals Inc. The detailed PLD parameters and process can be found in our previous publications.[12,43] Ta layer was introduced in a controlled way to interrupt the growth of the columnar structure of Cu, and to constraint the equi-axed Cu grains. The thicknesses of Cu and Ta layers were controlled by manipulating the exposure durations of Cu and Ta targets to the laser beam.

X-ray diffraction (XRD) analysis was carried out using a Rigaku X-ray diffractometer with Cu-K α radiation ($\lambda = 0.154$ nm). XRD θ - 2θ scan patterns were utilized to determine the out-of-plane orientation and planar spacing

of the Cu films, based on which the in-plane and out-of-plane strain of Cu films were calculated. Si (400) peaks were used as the internal reference standard for the estimation of strain. The strains for Si/Cu systems are limited to regions of the order of 10 nm, close to the Cu/Si interface. Since XRD probes distances of the order of microns, the Si (400) peaks can provide the internal standard without being affected by interfacial strains. These strains will contribute slightly to the width of the peak, but the positions of Si (400) peaks will remain unchanged. The microstructures of these films were characterized using a JEOL-2000FX transmission electron microscope (TEM). Twins in Cu films and NC Cu grains were observed from the cross-section of the film using a JEOL-2010F high-resolution TEM (HRTEM), equipped with a Gatan image filter tuning attachment, which has a point-to-point resolution of 0.18 nm. The sample for TEM observation was prepared using conventional sample preparation techniques including mechanical polishing, dimpling, and Ar ion milling by using the Precision Ion Polishing System at a beam energy of 5 keV, incidence angle of 5° during the initial stage and beam energy of 3 keV, incidence angle of 2° during the final stage. The sample for HRTEM observation was further ion-milled for 15 min at a beam energy of 3 keV and incidence angle of 1° .

Texture and Stress State of the Cu Film XRD analysis was used to determine the texture and residual stress of the Cu films. Figure 1 shows the XRD θ - 2θ scan patterns for five different Cu/Ta multilayer films integrated on Si substrates. Only a single Cu $\{111\}$ peak appears in these five patterns, indicating that the NC Cu grains inside these multilayer films are highly textured with the $\{111\}$ planes parallel to the film surface. However, the position of the $\{111\}$ peak varies from sample to sample, suggesting a variation in the spacing of the $\{111\}$ planes that are parallel to the surface. Take film 1 as an example,

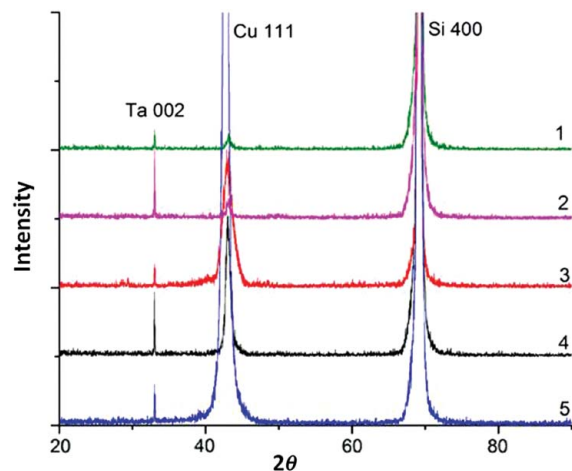


Figure 1. XRD θ - 2θ scan patterns for five different Cu/Ta multilayer films integrated on Si substrates.

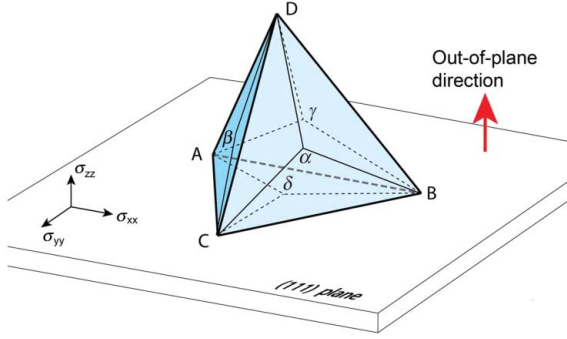


Figure 2. Schematic illustration of σ_{xx} , σ_{yy} , σ_{zz} and different $\{111\}$ planes of Cu within the multilayer structure.

the Cu $\{111\}$ peak is measured to be located at the position of $2\theta = 43.0869^\circ$. According to the Bragg Law ($2d \sin\theta = \lambda$), the planar spacing of Cu $\{111\}$ planes parallel to the surface is calculated to be $d_{//} = 2.0977 \text{ \AA}$. Consequently, the lattice constant of Cu along the out-of-plane direction is $a_{zz} = \sqrt{3}d_{//} = 3.6333 \text{ \AA}$. Since the standard lattice constant of Cu is 3.610 \AA , the out-of-plane strain ε_{zz} of the Cu film can thus be calculated to be 0.6448% (see Figure 2 for the orientation of coordinates).

According to the generalized relationship between stress and strain tensors in cubic crystals,[44] the stresses and strains along different directions are related with each other.[45] Combine these relationships with the equation among the out-of-plane strain ε_{zz} , in-plane strain ε_{xx} , ε_{yy} , and Poisson's ratio ν , i.e. $(\varepsilon_{zz}/(\varepsilon_{xx} + \varepsilon_{yy})) = -\nu/(1 - \nu)$,[45] we can obtain the in-plane and out-of-plane stresses in film 1: $\sigma_{xx} = \sigma_{yy} = -1.17 \text{ GPa}$, and $\sigma_{zz} = 0 \text{ GPa}$. This routine procedure to calculate in-plane and out-of-plane stresses in thin films from out-of-plane strain can also be found in the text.[46] Note that these values calculated from X-ray data may not be very accurate and can only be considered qualitative. The residual stress in thin film heterostructures results from three sources: lattice mismatch, thermal mismatch, and defects.[45] Since the Cu films are not epitaxial layers on Si and the PLD depositions were conducted at room temperature, thermal and lattice mismatches cannot be the strain sources for Cu films in this case. Consequently, the accumulated compressive in-plane stresses within Cu films are due to defects in the Cu layers or at the Cu/Ta interfaces.

The orientations of σ_{xx} , σ_{yy} , σ_{zz} and different $\{111\}$ planes of Cu within the multilayer structure are illustrated in Figure 2. Since σ_{xx} , σ_{yy} , and σ_{zz} are all normal stresses, the Shockley partial dislocations on ABC plane cannot glide. However, since planes BCD, ABD, and ACD form an angle of 70.5° with plane ABC, the shear components of σ_{xx} , σ_{yy} , and σ_{zz} will encourage the partial dislocations to glide on them and possibly generate twins. Consider plane BCD in film 1 as an example, the shear stress on Shockley partial $\alpha\mathbf{D}$ can be calculated as

1.10 GPa , which is much higher than the stress needed to activate twinning.[47] Therefore, the twins observed here are deformation twins. In addition, the statistical grain size effect on the twin density also indicates that the twins in the NC Cu are mostly deformation twins.[43] The shear stresses on Shockley partial dislocations $\beta\mathbf{\alpha}$ or $\mathbf{C}\alpha$ are 0.55 GPa , which is close to the critical shear stress. Therefore, for the majority of NC Cu grains in these multilayer films, the emission and slip of $\alpha\mathbf{D}$ partial dislocations will be dominant on the BCD planes. For the same reason, $\beta\mathbf{D}$ partial dislocations will be dominant on the ACD planes and $\gamma\mathbf{D}$ partial dislocations will be dominant on the ABD planes. This indicates that the strain condition within our films drives the CSTP mechanism and the MAP mechanism, while suppressing the RAP mechanism.

Microstructure in the Cu/Ta Film Figure 3(a) shows the cross-sectional dark field (DF) image of a Cu/Ta/Si multilayer structure, in which 26 layers of thin Cu films are separated by 25 much thinner layers of Ta. The Cu grains inside each layer of the film were constrained by the thin Ta layers, such that columnar growth of Cu was interrupted and a majority of near equi-axed NC grains were obtained. In addition, the grain rotation and grain boundary sliding in the NC Cu are confined by the Ta layers, making it difficult for them to rotate along the thickness direction. Figure 3(b) is the cross-sectional DF image of another Cu/Ta/Si multilayer structure, in which 50 layers of NC Cu are separated by 49 much thinner layers of Ta. Based on the TEM observation of the as-grown Cu/Ta/Si multilayer structures, we found that the majority of the NC Cu grains were equi-axed and the grain sizes of these NC Cu grains range from ~ 10 to $\sim 80 \text{ nm}$. The layer thicknesses and grain size ranges for films 1–5 are summarized in Table 1. A typical $\langle 110 \rangle$ zone-axis selected area diffraction pattern (SADP) of one Si/Cu/Ta multilayer heterostructure is shown in Figure 3(c). The $\langle 110 \rangle$ zone-axis pattern of Si reveals the single-crystal nature of the substrate. However, the scattered diffraction points on the red circle shows that Cu layers are $\{111\}$ textured. Ta layers are too thin to show visible diffraction spots on the SADP. Figure 3(d) is the corresponding HRTEM image showing the structure of Cu/Ta layers and the interface morphology. The Ta layers appear

Table 1. The layer thicknesses and grain size ranges for films 1–5.

| Film | Layer thickness (nm) | Grain size range (nm) |
|------|----------------------|-----------------------|
| #1 | 6–18 | 5–20 |
| #2 | 20–30 | 18–30 |
| #3 | 45–49 | 30–50 |
| #4 | 62–66 | 50–68 |
| #5 | 80–85 | 60–85 |

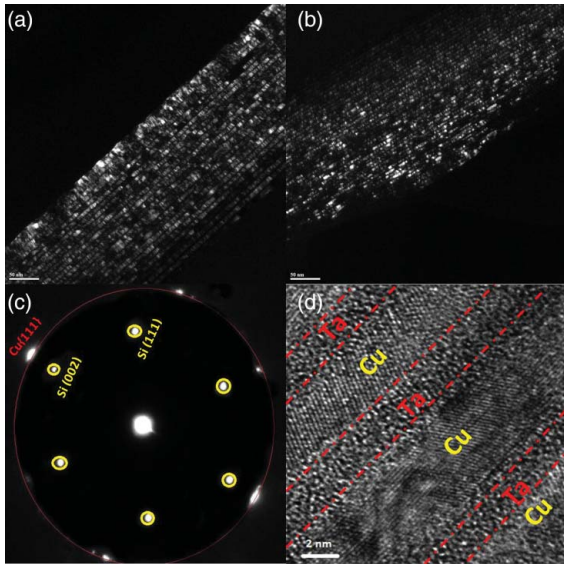


Figure 3. (a) Cross-sectional DF image of a typical Cu/Ta multilayer film on Si substrate; (b) cross-sectional DF image of another Cu/Ta multilayer structure on Si substrate; (c) the typical $\langle 110 \rangle$ zone-axis SADP of the Si/Cu/Ta multilayer heterostructure. Cu layers are $\{111\}$ textured, while Ta layers are too thin to show diffraction spots on the SADP. (d) The typical HRTEM image showing the structure of Cu/Ta layers and the interface morphology.

darker than Cu layers due to mass contrast, which results from the higher atomic number of Ta. Ta layers are only a few monolayers thick, and their crystal structure is highly defected. The interfaces between Cu and Ta layers are clean and smooth. As shown, each Cu layer is made of a monolayer of Cu grains between adjacent Ta layers. Ta can effectively prevent Cu diffusion, because Cu and Ta are almost completely immiscible and will not react to form any compounds according to their phase diagram.[48]

The reason for the activation of the RAP [23] has been attributed to the unique deformation behavior of NC materials, i.e. variation with time of the local shear stresses.[23] The grain boundary sliding and grain rotation can alter local stress state [49] or change the orientation of the twinned grain, which can promote the random emission of partial dislocations.[23] In our NC Cu/Ta films, the Cu–Ta interface restricts the rotation of the Cu grains, which consequently suppresses the RAP mechanism.

Twins with Zero-Macrostrain Twins with zero macroscopic strain can be identified by the smooth grain boundary segments at locations where they intersect the TBs.[23] Figure 4 shows HRTEM images of typical NC Cu grains containing twins with zero macroscopic strain. In Figure 4(a), Shockley partials were emitted from the grain boundary, which glided on successive $\{111\}$ planes across the whole grain to the other side of the grain.

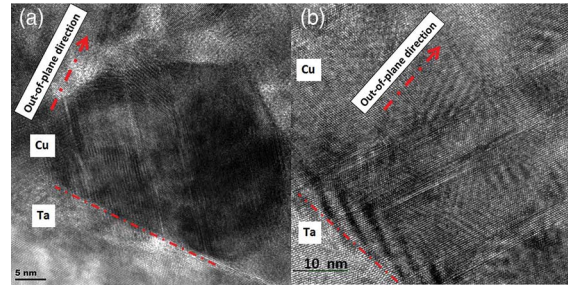


Figure 4. Typical NC Cu twinned grains with zero macroscopic strains, as manifested by smooth grain boundaries. The out-of-plane direction is shown by the arrow.

The grain boundary was smooth at the intersection locations with TBs, indicating a zero macroscopic strain. In Figure 4(b), the Shockley partials were emitted from the grain boundary and glided on successive $\{111\}$ planes but terminated inside the grain. Despite of some Moire fringes on the left side of the grain boundary, no shape change of the grain boundary occurred, indicating again a zero macroscopic strain associated with the twinning process. Considering that RAP mechanism [18] has been suppressed in our films, the zero-macrostrain twins were more likely to be formed via the CSTP mechanism, in which groups of three Shockley partial dislocations with different Burgers vectors cooperatively glide.[35] Assuming \mathbf{b}_1 , \mathbf{b}_2 , and \mathbf{b}_3 are the three possible Shockley partial dislocations in a group, then $\mathbf{b}_1 + \mathbf{b}_2 + \mathbf{b}_3 = \mathbf{0}$.

Twins with Macrostrain Most twins in our films were found to generate macroscopic strains, as manifested by the shape change of grain boundaries. To study the occurring frequencies of twinning with and without macrostrain, we observed 54 grains containing twins, among which 24 have smooth grain boundaries and the other 30 have kink angles on their boundaries. In other words, macrostrains were generated in $\sim 56\%$ of the twinned grains due to the twinning process, which is in sharp contrast with previous reports in NC materials.[23, 35–39] This result shows that with RAP suppressed, zero-macrostrain twins cease to dominate in our NC Cu grains. This indirectly proves that the RAP mechanism played a significant role in producing deformation twins with zero-macrostrain. The result also means that the CSTP mechanism accounted for at least 44% of the deformation twins with zero-macrostrain in the current experiment, suggesting that CSTP should be also a major mechanism for producing deformation twins with zero-macrostrain.

The activation condition of the RAP mechanism is different from that of the CSTP [35–39] mechanism. The former requires the dynamic change in stress orientation so that partials with different Burgers vectors can be activated randomly from the grain boundaries. In contrast, if

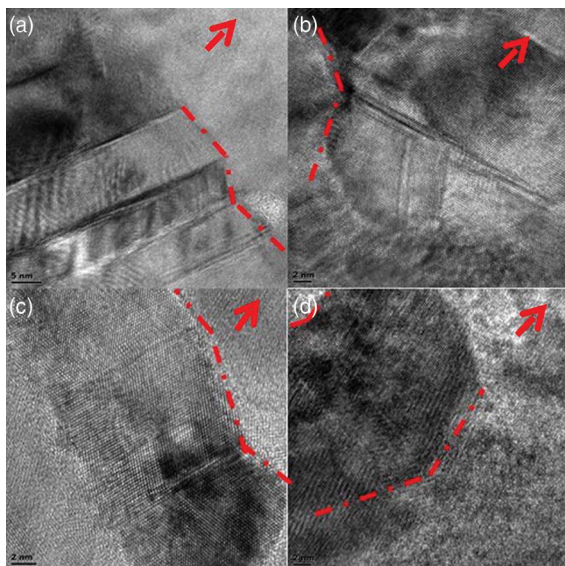


Figure 5. Typical NC Cu twinned grains with macroscopic strains, as manifested by shape change (kink angles) on grain boundaries. The out-of-plane direction for each part of the image is shown by the arrow.

the local stress remains unidirectional without change in orientation, the MAPs will be favored to produce macroscopic twinning strain, while at the same time the CSTP mechanism will be also favored to produce twins with zero-macrostrain, as observed in this experiment. During the deformation of a conventional bulk NC fcc metal, some grains may rotate. In other words, both RAP and CSTP are likely the major mechanisms for producing deformation twins with zero-macrostrain.

Figure 5 shows typical NC Cu grains in which macroscopic strains were generated by twins. In Figure 5(a), multiple twins are adjacent to each other and a large shear strain exists at each location where the TB intersects with the grain boundary. Two kink angles of the shear-strained grain boundary can be readily measured, where the upper kink angle is $145^\circ \pm 2^\circ$ and the lower kink angle is close to 141° . In Figure 5(b), there is only one kink angle on the grain boundary and it is found to be close to 141° . Figure 5(c) shows an elongated grain whose width (i.e. the distance between the left and right sides of the grain) is about 14 nm. Two twins are adjacent to each other and the Shockley partial dislocations were emitted from one side of the grain boundary and glided across the whole grain to reach the other side of the grain boundary. A grain boundary kink exists at each location where the TB intersects with the grain boundary. The upper grain boundary kink angle is $157^\circ \pm 2^\circ$, and the lower kink angle is close to 141° . Figure 5(d) shows a ~ 35 nm NC Cu grain in which one TB intersects with both the top and bottom sides of the grain boundary, generating a macroscopic strain. Both the upper and lower kink angles are close to 141° .

The macrostrain of the grains containing twins can be generated through two mechanisms:

- (1) The MAP,[23] in which twinning partials with the same Burgers vector are emitted on every slip plane at the grain boundary to generate a twin with a large macroscopic strain.[50] For such a twin, the grain boundary kink angle will be 141° if viewed from the $\langle 110 \rangle$ orientation that perpendicular to the Burgers vector of the twinning partial, and it will be 158° if viewed from other possible $\langle 110 \rangle$ orientations [50].
- (2) The emission of partial dislocations with two different Burgers vectors, in which twinning partials with two different Burgers vectors are emitted alternatively at the grain boundary, such that the net sum of their Burgers vectors is equal to that of only one partial dislocation, and a twin with smaller shear strain is generated.[50] The grain boundary kink angle will be 158° if viewed from the $\langle 110 \rangle$ orientation that perpendicular to the net sum of the two Burgers vectors of the twinning partial dislocations, and it will be 169° if viewed from other possible $\langle 110 \rangle$ orientations.[50]

It is also possible to form a twin by the mixture of the first and second mechanisms.[50] According to the above rationale, most of the twins in Figure 5 are formed by the MAP mechanism, while some may be formed by the second mechanism or a mixture of the two.

In summary, we have carefully designed the Cu/Ta multilayer structure to obtain a texture and stress state to promote the MAPs with the same Burgers vector and the cooperative slip of three partials. The confinement of grain boundary rotations helps maintain the local stress condition, such that the RAP is suppressed. The results indicate that MAP dislocations with the same Burgers vector dominate twin formation under monotonic stress. The results also suggest that both the RAP and the CSTP are significant mechanisms for forming the previously reported zero-macrostrain twins in NC fcc metals.

Acknowledgements We acknowledge the support by the National Science Foundation of the USA (Grant No. DMR-1104667). We also acknowledge the use of the Analytical Instrumentation Facility (AIF) at North Carolina State University, which is supported by the State of North Carolina and the National Science Foundation.

References

- [1] Cheng GM, Xu WZ, Jian WW, Yuan H, Tsai MH, Zhu YT, Zhang YF, Millett PC. Dislocations with edge components in nanocrystalline bcc Mo. *J Mater Res.* 2013;28(13):1820–1826.

- [2] Zhu YT, Liao XZ, Wu XL. Deformation twinning in nanocrystalline materials. *Prog Mater Sci*. 2012;57(1):1–62.
- [3] Liao XZ, Zhou F, Lavernia EJ, Srinivasan SG, Baskes MI, He DW, Zhu YT. Deformation mechanism in nanocrystalline Al: partial dislocation slip. *Appl Phys Lett*. 2003;83(4):632–634.
- [4] Zhu YT, Narayan J, Hirth JP, Mahajan S, Wu XL, Liao XZ. Formation of single and multiple deformation twins in nanocrystalline fcc metals. *Acta Mater*. 2009;57(13):3763–3770.
- [5] Narayan J, Zhu YT. Self-thickening, cross-slip deformation twinning model. *Appl Phys Lett*. 2008;92(15):151908.
- [6] Chen K-C, Wu W-W, Liao C-N, Chen L-J, Tu KN. Observation of atomic diffusion at twin-modified grain boundaries in copper. *Science*. 2008;321(5892):1066–1069.
- [7] Lu L, Shen Y, Chen X, Qian L, Lu K. Ultrahigh strength and high electrical conductivity in copper. *Science*. 2004;304(5669):422–426.
- [8] Liao XZ, Huang JY, Zhu YT, Zhou F, Lavernia EJ. Nanostructures and deformation mechanisms in a cryogenically ball-milled Al-Mg alloy. *Philos Mag*. 2003;83(26):3065–3075.
- [9] Lu K, Lu L, Suresh S. Strengthening materials by engineering coherent internal boundaries at the nanoscale. *Science*. 2009;324(5925):349–352.
- [10] Wang YB, Sui ML. Atomic-scale in situ observation of lattice dislocations passing through twin boundaries. *Appl Phys Lett*. 2009;94(2):021909.
- [11] Wang YB, Wu B, Sui ML. Dynamical dislocation emission processes from twin boundaries. *Appl Phys Lett*. 2008;93(4):041906.
- [12] Wu F, Wen HM, Lavernia EJ, Narayan J, Zhu YT. Twin intersection mechanisms in nanocrystalline fcc metals. *Mater Sci Eng A*. 2013;585(0):292–296.
- [13] Cao Y, Wang YB, Liao XZ, Kawasaki M, Ringer SP, Langdon TG, Zhu YT. Applied stress controls the production of nano-twins in coarse-grained metals. *Appl Phys Lett*. 2012;101(23):231903–231905.
- [14] Ni S, Wang YB, Liao XZ, Figueiredo RB, Li HQ, Ringer SP, Langdon TG, Zhu YT. The effect of dislocation density on the interactions between dislocations and twin boundaries in nanocrystalline materials. *Acta Mater*. 2012;60(6–7):3181–3189.
- [15] Afanasyev KA, Sansoz F. Strengthening in gold nanopillars with nanoscale twins. *Nano Lett*. 2007;7(7):2056–2062.
- [16] Henager CH Jr, Hoagland RG. A rebound mechanism for misfit dislocation creation in metallic nanolayers. *Scripta Mater*. 2004;50(5):701–705.
- [17] Jin J, Shevlin SA, Guo ZX. Multiscale simulation of onset plasticity during nanoindentation of Al (001) surface. *Acta Mater*. 2008;56(16):4358–4368.
- [18] Yamakov V, Wolf D, Phillpot SR, Gleiter H. Dislocation–dislocation and dislocation–twin reactions in nanocrystalline Al by molecular dynamics simulation. *Acta Mater*. 2003;51(14):4135–4147.
- [19] Ma E, Wang YM, Lu QH, Sui ML, Lu L, Lu K. Strain hardening and large tensile elongation in ultrahigh-strength nano-twinned copper. *Appl Phys Lett*. 2004;85(21):4932–4934.
- [20] Zhao YH, Bingert JE, Liao XZ, Cui BZ, Han K, Sergueeva AV, Mukherjee AK, Valiev RZ, Langdon TG, Zhu YTT. Simultaneously increasing the ductility and strength of ultra-fine-grained pure copper. *Adv Mater*. 2006;18(22):2949–2953.
- [21] Wang ZW, Wang YB, Liao XZ, Zhao YH, Lavernia EJ, Zhu YT, Horita Z, Langdon TG. Influence of stacking fault energy on deformation mechanism and dislocation storage capacity in ultrafine-grained materials. *Scripta Mater*. 2009;60(1):52–55.
- [22] Zhao YH, Liao XZ, Horita Z, Langdon TG, Zhu YT. Determining the optimal stacking fault energy for achieving high ductility in ultrafine-grained Cu-Zn alloys. *Mater Sci Eng A*. 2008;493(1–2):123–129.
- [23] Wu XL, Liao XZ, Srinivasan SG, Zhou F, Lavernia EJ, Valiev RZ, Zhu YT. New deformation twinning mechanism generates zero macroscopic strain in nanocrystalline metals. *Phys Rev Lett*. 2008;100(9):095701.
- [24] Zhao YH, Zhu YT, Liao XZ, Horita Z, Langdon TG. Tailoring stacking fault energy for high ductility and high strength in ultrafine grained Cu and its alloy. *Appl Phys Lett*. 2006;89(12):121906.
- [25] Yamakov V, Wolf D, Phillpot SR, Mukherjee AK, Gleiter H. Deformation-mechanism map for nanocrystalline metals by molecular-dynamics simulation. *Nat Mater*. 2004;3(1):43–47.
- [26] Yamakov V, Wolf D, Phillpot SR, Mukherjee AK, Gleiter H. Dislocation processes in the deformation of nanocrystalline aluminium by molecular-dynamics simulation. *Nat Mater*. 2002;1(1):45–48.
- [27] Yamakov V, Wolf D, Phillpot SR, Gleiter H. Grain-boundary diffusion creep in nanocrystalline palladium by molecular-dynamics simulation. *Acta Mater*. 2002;50(1):61–73.
- [28] Chen MW, Ma E, Hemker KJ, Sheng HW, Wang YM, Cheng XM. Deformation twinning in nanocrystalline aluminum. *Science*. 2003;300(5623):1275–1277.
- [29] Liao XZ, Zhou F, Lavernia EJ, He DW, Zhu YT. Deformation twins in nanocrystalline Al. *Appl Phys Lett*. 2003;83(24):5062–5064.
- [30] Liao XZ, Zhao YH, Srinivasan SG, Zhu YT, Valiev RZ, Gunderov DV. Deformation twinning in nanocrystalline copper at room temperature and low strain rate. *Appl Phys Lett*. 2004;84(4):592–594.
- [31] Wu XL, Ma E. Deformation twinning mechanisms in nanocrystalline Ni. *Appl Phys Lett*. 2006;88(6):061905.
- [32] Wang YM, Hodge AM, Biener J, Hamza AV, Barnes DE, Liu K, Nieh TG. Deformation twinning during nanoindentation of nanocrystalline Ta. *Appl Phys Lett*. 2005;86(10):101915.
- [33] Rosner H, Markmann J, Weissmuller J. Deformation twinning in nanocrystalline Pd. *Philos Mag Lett*. 2004;84(5):321–334.
- [34] Wu XL, Zhu YT. Inverse grain-size effect on twinning in nanocrystalline Ni. *Phys Rev Lett*. 2008;101(2):025503.
- [35] Wang J, Anderoglu O, Hirth JP, Misra A, Zhang X. Dislocation structures of Sigma 3 {112} twin boundaries in face centered cubic metals. *Appl Phys Lett*. 2009;95(2):021908.
- [36] Wang J, Li N, Anderoglu O, Zhang X, Misra A, Huang JY, Hirth JP. Detwinning mechanisms for growth twins in face-centered cubic metals. *Acta Mater*. 2010;58(6):2262–2270.
- [37] Wang J, Misra A, Hirth JP. Shear response of Sigma 3 {112} twin boundaries in face-centered-cubic metals. *Phys Rev B*. 2011;83(6):064106.
- [38] Liu L, Wang J, Gong SK, Mao SX. High resolution transmission electron microscope observation of zero-strain deformation twinning mechanisms in Ag. *Phys Rev Lett*. 2011;106(17):175504.
- [39] Li BQ, Li B, Wang YB, Sui ML, Ma E. Twinning mechanism via synchronized activation of partial

- dislocations in face-centered-cubic materials. *Scripta Mater.* 2011;64(9):852–855.
- [40] Chinh NQ, Szommer P, Horita Z, Langdon TG. Experimental evidence for grain-boundary sliding in ultrafine-grained aluminum processed by severe plastic deformation. *Adv Mater.* 2006;18(1):34–39.
- [41] Liao XZ, Kilmametov AR, Valiev RZ, Gao HS, Li XD, Mukherjee AK, Bingert JF, Zhu YT. High-pressure torsion-induced grain growth in electrodeposited nanocrystalline Ni. *Appl Phys Lett.* 2006;88(2):021909.
- [42] Wang YB, Ho JC, Liao XZ, Li HQ, Ringer SP, Zhu YT. Mechanism of grain growth during severe plastic deformation of a nanocrystalline Ni-Fe alloy. *Appl Phys Lett.* 2009;94(1):011908.
- [43] Wu F, Zhu YT, Narayan J. Grain size effect on twin density in as-deposited nanocrystalline Cu film. *Philos Mag.* 2013; (in press).
- [44] JP Hirth, Lothe J. *Theory of dislocations.* New York: McGraw-Hill; 1968.
- [45] Narayan J. Recent progress in thin film epitaxy across the misfit scale (2011 Acta Gold Medal Paper). *Acta Mater.* 2013;61(8):2703–2724.
- [46] Freund SSLB, editor. *Thin film materials: stress, defect formation, and surface evolution.* New York: Cambridge University Press; 2003.
- [47] Zhu YT, Liao XZ, Srinivasan SG, Lavernia EJ. Nucleation of deformation twins in nanocrystalline face-centered-cubic metals processed by severe plastic deformation. *J Appl Phys.* 2005;98(3):034319.
- [48] Kaloyeros AE, Eisenbraun E. Ultrathin diffusion barriers/liners for gigascale copper metallization. *Annu Rev Mater Sci.* 2000;30(1):363–385.
- [49] Meyers MA, Mishra A, Benson DJ. Mechanical properties of nanocrystalline materials. *Prog Mater Sci.* 2006;51(4):427–556.
- [50] Zhu YT, Wu XL, Liao XZ, Narayan J, Mathaudhu SN, Kecskes LJ. Twinning partial multiplication at grain boundary in nanocrystalline fcc metals. *Appl Phys Lett.* 2009;95(3):031909.